Effects of pH and Calcium Ions on the Conformational Transitions in Silk Fibroin Using 2D Raman Correlation Spectroscopy and ^{13}C Solid-State NMR†

Ping Zhou,*,‡ Xun Xie,‡ David P. Knight,§ Xiao-Hong Zong,‡ Feng Deng,|| and Wen-Hua Yao⊥

The Key Laboratory of Molecular Engineering of Polymers, Ministry of Education, Department of Macromolecular Science, Fudan University, Shanghai 200433, China, Zoology Department, University of Oxford, South Parks Road, Oxford OX1 3PS, U.K., The State Key Laboratory of Magnetic Resonance and Atomic and Molecular Physics, Wuhan Institute of Physics & Mathematics, The Chinese Academy of Sciences, Wuhan 430071, China, and The Analytical Measurement Center, Fudan University, Shanghai 200433, China

Received April 5, 2004; Revised Manuscript Received June 30, 2004

ABSTRACT: Silk fibroin exists in a number of different states, such as silk I and silk II, with different properties largely defined by differences in secondary structure composition. Numerous attempts have been made to control the transitions from silk I to silk II in vitro to produce high-performance materials. Of all the factors influencing the structural compositions, pH and some metal ions play important roles. This paper focuses on the influence of pH and Ca^{2+} ions on the conformational transition from silk I to silk II in regenerated (redissolved) *Bombyx mori* fibroin. One- and two-dimensional correlation Raman spectroscopy was used to describe qualitatively the transitions in secondary structure in silk I, silk II, and their intermediates as pH and Ca^{2+} ion concentration were changed, while ^{13}C cross polarization magic angle spinning (CP/MAS) solid-state NMR was used to quantify these changes. We showed that conditions (low pH, pH 5.2; a defined range of Ca^{2+} ion concentrations; gradual water removal) that mimic natural silk spinning promote the formations of β-sheet and distorted β-sheet characteristic of silk II or silk II-related intermediate. In contrast, higher pH (pH 6.9−8.0) and higher Ca^{2+} ion concentrations maintain "random coil" conformations typical of silk I or silk I-related intermediate. These results help to explain why the natural silk spinning process is attended by a reduction in pH from 6.9 to 4.8 and a change in the Ca^{2+} ion concentration in the gland lumen as fibroin passes from the posterior division through the secretory pathway to the anterior division.

Bombyx mori heavy chain fibroin, a major structural protein of silk, is largely composed of repeats of the motif $(Gly\text{-}Ala\text{-}Gly\text{-}Ala\text{-}Gly\text{-}Ser)_n$ (*1*). Within the lumen of the posterior and middle divisions of the gland, the heavy chain fibroin is thought to be present as a silk I-like conformation lacking ordered secondary structure (*2*) and largely containing extended chains repeatedly folded back on themselves (*3*−*5*). During natural spinning, this conformation is thought to be converted into silk II, which is largely formed from crystalline β-sheets (*6*). These β-sheets are well orientated along the axis of the fiber (*7*) except for the short disordered regions, giving it a strength and stiffness comparable or even superior to that of high-performance synthetic materials (*8*−*10*). The fact that silk filaments are formed naturally under physiological conditions at ambient temperatures, without high hydrostatic pressure, and without the use of toxic solvents has prompted us to inquire into the factors responsible for the structural transition(s) involved in this remarkable process.

It is now possible, through recombinant DNA technology, to genetically engineer *Escherichia coli* bacteria to produce silk-like proteins with precisely specified amino acid sequences (*11*−*13*). Recently, Lazaris et al. (*14*) also produced soluble recombinant (rc) silk proteins with molecular masses of 60−140 kDa by expressing the dragline silk genes (ADF-3/MaSpII and MaSpI) of two spider species in mammalian cells. These were then extruded as monofilaments from a concentrated aqueous solution of soluble rc spider silk protein using alcohol coagulation. However, these filaments lack the tenacity of natural dragline silks (*14*). This may stem from the well demonstrated fact that the properties of naturally formed silk fibers depend not only on their chemical composition but also on their nanocomposite construction (*15*, *16*) and on the pH, water content and element composition (microenvironment) during spinning (*8*−*30*). The importance of processing conditions in the definition of mechanical properties is highlighted by the observation that artificially reeling silk from immobilized silkworms at a constant rate produced fibers that were superior to naturally spun ones (*10*). This probably resulted from the variable spinning speed and tension in natural spinning, a consequence of the side-to-side movement of the silkworm's head (*10*). The silkworm produces stronger, more brittle fibers at faster

† Supported by grants from the NSFC (Nos. 20274009 and 29974004) and from The State Key Laboratory of Magnetic Resonance and Atomic and Molecular Physics, China.

* To whom correspondence should be addressed. Phone: +86-21-55664038. Fax: +86-21-65640293. E-mail: pingzhou@fudan.edu.cn.

‡ Department of Macromolecular Science, Fudan University.

§ University of Oxford.

|| Wuhan Institute of Physics and Mathematics, The Chinese Academy of Sciences.

⊥ The Analytical Measurement Center, Fudan University.

10.1021/bi049344i CCC: $27.50
Published on Web 08/12/2004

spinning speeds, whereas slower speeds lead to weaker, more extensible fibers (*10*).

Further evidence of the importance of processing conditions was obtained by Seidel and collaborators (*17*, *18*). They produced an "artificial" silk spun from spider silk dissolved in hexafluoro-2-propanol. The tensile properties of this material were shown to be affected by the extent of draw applied to it during processing. These authors also showed that water plasticized the silk fibroin facilitating protein crystallization during the postspin drawing processes.

Changes in element composition and pH as the silk dope passes through the spinning duct have been investigated in *Nephila senegalensis* spiders (*19*) and in *Bombyx mori* silkworms (*20*). The pH changes progressively from pH 6.9 to 6.3 in the spider dragline silk spinning duct (*19*) and from pH 6.9 to 4.8 in the silkworm (*20*). In both cases, it has been suggested that metal cations help in some way to refold the silk protein molecules while the secretion of H^+ may assist in this process by changing the ionization of charged groups on the protein (*19*). In silkworms, shearing in the silk press and extensional flow produced by moving the head when spinning are also thought to facilitate the formation of β-sheet (*21*, *22*).

There are several reports concerning the effect of pH and metal ions on silk fibroin conformations (*23*−*30*). Magoshi et al. (*27*) found that silkworm formed fibers from the nematic liquid crystalline state, which was transformed from a gel state to a sol state in the anterior division of the gland. The viscosity, pH, and freezing point depression fell from the posterior division of gland to the anterior division, while the Ca^{2+} ion concentration increased somewhat. Recently, these authors investigated the effect of Ca^{2+} ion concentration based on the rheology and dynamic light scattering of silk fibroin in posterior division (P) and posterior (MP), middle (MM), and anterior (MA) parts of the middle division of *Bombyx mori* silkworm (*29*, *30*). They found that Ca^{2+} ion concentrations increased from P division to MM part and then decreased in the MA part of middle division, inducing a sol−gel conversion coupled with molecular aggregation. Thiel and Viney (*26*) used inductively coupled plasma mass spectrometry (ICP-MS) to investigate the effect of spinning rate on the metal ion contents of spider dragline filaments. Fast spinning produced a marked reduction in the Ca^{2+} ion content of the silk filament. They speculated that the metal ion Ca^{2+} facilitated the formation of β-sheet (*28*). They claimed that Ca^{2+} was exclusively located in the β-sheet crystallites, but their evidence from transmission electron microscopy is open to other interpretations. They also speculated on the possible role of calcium in stabilizing (or even nucleating) the crystalline component of silk fiber microstructures. Li et al. (*25*) investigated the effect of K^+, Ca^{2+}, Cu^{2+}, and Zn^{2+} ions on the secondary structures of silkworm fibroin, reporting that all these ions at certain concentrations could promote the random coil to β-sheet transition.

Although the above observations strongly suggest that reduction in pH and an increase in the defined concentration of some metal ions could induce the β-sheet conformation, the effect of different concentrations of these ions on the kinetics of this transition has not been elucidated. Understanding these issues would provide further insight into the refolding mechanism of this remarkable protein with relevance to natural and biomimetic spinning. Accordingly, we report here the effects of pH, Ca^{2+} ion concentration, and water removal on the conformational transition in a model silk protein, regenerated silk fibroin.

Raman spectroscopy is a powerful and speedy method for studying the secondary structure of silk fibroin qualitatively (*31*, *32*, *33*). On the other hand, ^{13}C solid-state NMR is widely used to analyze quantitatively the protein secondary structure (*34*−*36*). Accordingly we used Raman spectroscopy as a rapid way of identifying secondary components in the fibroin together with ^{13}C cross polarization magic angle spinning (CP/MAS) NMR to quantify these components.

MATERIALS AND METHODS

Sample Preparation. Bombyx mori cocoons were degummed in boiling aqueous Na_2CO_3 (0.5 wt %) solution for half an hour. After thorough rinsing, the regenerated silk fibroin solution was prepared by dissolving 10 g of degummed silk in a 100 mL of 9.3 M LiBr solution for 1 h at room temperature. The resulting solution was dialyzed against deionized water at ambient temperature for 3 days to remove LiBr. The deionized water was changed every 4 h during dialysis. This yielded a 4 wt % silk fibroin stock solution. This was used to prepare 1 wt % regenerated fibroin solutions at a pH of 5.2, 6.9, and 8.0 by mixing equivalent volumes of 2 wt % fibroin solution and NaH_2PO_4−Na_2HPO_4 buffer with the defined pH values.

Fibroin solutions containing different concentrations of Ca^{2+} ion at different pHs were prepared by mixing 1 wt % fibroin buffer solutions with desired pH and different volumes of 0.01 M $CaCl_2$ aqueous bulk solutions to give defined Ca^{2+} ion concentrations. The low solubility of $CaHPO_4$ made it impossible to add Ca^{2+} ion to phosphate-buffered fibroin at a pH of 8.0, so different volumes of 0.01 M $CaCl_2$ solution were added to 1 wt % fibroin solution before adjusting the pH to 8.0 with 0.01 M NaOH and HCl solution while relying on the buffering capacity of the protein.

All the prepared solutions were left to dry at room temperature to form membranes on the polyester surfaces for about 3 days, partially imitating the process of water removal during natural spinning by the silkworm. The original Ca element content of dried regenerated silk fibroin membranes prepared in this way was found to be 1.040 ± 0.046 mg of Ca per gram of fibroin determined by particle induced X-ray emission (PIXE) (*25*), which is comparable to the Ca content in the dried contents of the lumen of the posterior division of the *Bombyx mori* silk gland as measured by Nemoto and co-workers (*30*). Accordingly, we prepared fibroin membranes containing about 1, 5, 10, 20, 50, and 100 times the original Ca content in the dried regenerated silk fibroin by adding 0, 5.0, 10.0, 20.0, 50.0, and 100.0 mg of Ca^{2+} per gram of fibroin into the fibroin solutions.

Raman Spectroscopy and Two-Dimensional Correlation Analysis. Raman spectra were recorded using a Dilor LabRam-1B spectrometer, operating at a resolution of 1 cm^{-1}. The Spectra Physics model 164 argon ion laser was operated at 632.8 nm with about 6 mW of power. The region of 1600−1700 cm^{-1} for amide I (stretching C=O) was investigated because of its high intensity and low interference from other molecular vibrations. In addition, this band has

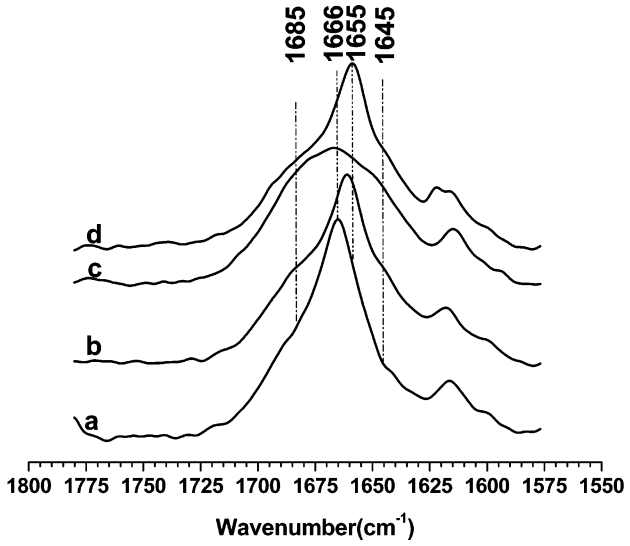

FIGURE 1: 1D Raman spectra of a series of membranes prepared from regenerated fibroin solutions buffered at pH 5.2 (a), 6.9 (c), and 8.0 (d) and from unbuffered solution at pH 6.6 (b) (see Materials and Methods section).

been widely used to distinguish β-sheet from random coil or α-helix in biological material (*37*) including silk fibroin (*31*, *32*). The following attributions are commonly employed: 1670 ± 5 cm^{-1} to β-sheet; 1660 ± 5 cm^{-1} to silk I or random coil conformation (*32*), and 1654 ± 5 cm^{-1} to α-helix (*37*).

Most of the Raman spectra that we observed were broad and of low resolution (Figure 1). We, therefore, used generalized two-dimensional correlation spectroscopy (*38*) to resolve the secondary structures in fibroin. This method is widely used recently in temperature- (*39*) and dynamics-dependent (*40*) spectroscopy to enhance effectively the spectral resolution and reveal details on the hydrogen bonding and conformational change that are not easily detected by the traditional one-dimensional spectroscopy. Both synchronous and asynchronous spectra (*38*) were used to follow qualitative changes in the secondary structure components. Two-dimensional correlation Raman spectra were analyzed by a 2D Pocha software composed by Daisuke Adachi (Department of Chemistry, Kwansei Gakuin University). 1D reference spectra were shown at the side and top of the 2D correlation maps for comparison (Figure 2). In the 2D correlation maps, unshaded regions indicate positive correlation intensities, while shaded regions indicate negative ones.

^{13}C CP-MAS NMR and Spectral Deconvolution. ^{13}C CP-MAS NMR experiments were carried out on prepared membranes using a Varian Infinityplus-400 spectrometer operated at 100 MHz with cross polarization contact time of 1 ms, pulse repeat time of 2 s, accumulation of 1000 scans, and high-power ^{1}H-decoupling of 62.5 kHz during signal acquisition with a ^{1}H 90° pulse width of 4.0 μs. Sample was spun at a rate of 5 kHz in a 7.5 mm spin rotor. Chemical shifts were reported relative to the external reference of methyl carbon (17.3 ppm) in hexamethylbenzene. The NMR peak of C_β (chemical shifts between 5 and 30 ppm) for alanine residue was deconvoluted using Gaussian functions to analyze quantitatively the secondary structure components (Figure 3) because this peak provides sensitive discrimination between silk I and silk II and other secondary structural components in fibroin (*34*−*36*). To prove the quantified results, we measured the longitudinal relaxation time T_1 of ^{13}C for the silk fibroin membrane and obtained a single-exponential decay with T_1 of 0.57 ± 0.03 s for the C_β nucleus. That implies that the components existing in the C_β peak may have similar dynamics. In addition, we also compared the lineshapes of C_β with pulse delays of 2 and 5 s, as well as with contact time from 0.8 to 1.2 ms. We found that there were identical lineshapes under these experimental parameters. Therefore, we thought it reliable to analyze quantitatively the components deconvoluted in the C_β peak.

RESULTS AND DISCUSSION

Influence of pH on Silk Fibroin Conformation. Figure 1 shows the Raman spectra of membranes prepared at different pH values. These broad and highly overlapped spectra include conformations corresponding to the peaks around 1645, 1655, 1666, and 1685 cm^{-1}. The peak around 1616 cm^{-1} is attributed to the residues of phenylalanine, tyrosine, and tryptophan (*32*). This peak was normalized for intensity

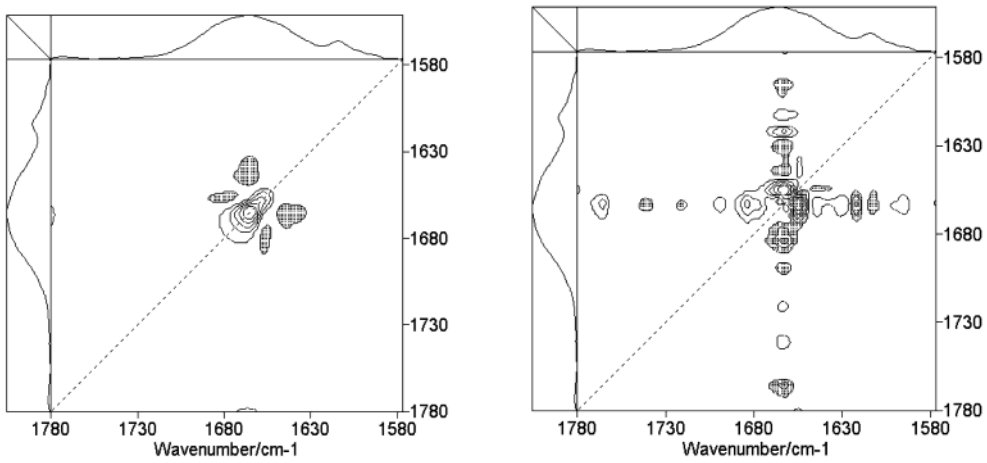

FIGURE 2: 2D synchronous (A) and asynchronous (B) Raman correlation spectra of silk fibroin corresponding to pH decrease from pH 8.0 to pH 5.2. Unshaded regions indicate positive correlation intensities, while shaded regions indicate negative correlation intensities.

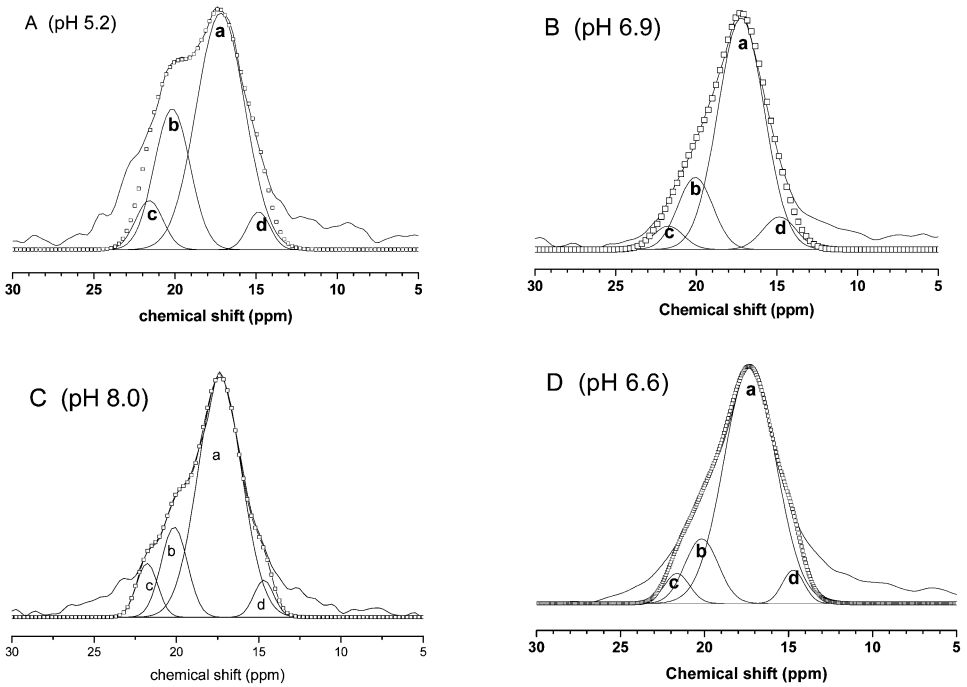

FIGURE 3: ^{13}C CP/MAS NMR spectra (solid line) and simulated ones (hollow squares) and their deconvoluted traces for alanine C_β. Membranes were prepared from regenerated fibroin solutions buffered at pH 5.2 (A), 6.9 (B), and 8.0 (C) and from unbuffered solution at pH 6.6 (D) (see Materials and Methods section). Deconvolution gives typical silk I (17.0 ± 0.5 ppm, a), typical silk II (20.0 ± 0.5 ppm, b), silk II-related intermediate (21.5 ± 0.5 ppm, c), and silk I-related intermediate (15.0 ± 0.5 ppm, d).

comparison during the study for the Raman spectra. Among these spectra, Figure 1b shows the spectrum of a membrane prepared from the original regenerated silk fibroin solution (pH 6.6) without phosphate buffering. The peak intensity at 1666 cm^{-1} has been assigned to a silk II (β-sheet) conformation and the peak at 1655 cm^{-1} to a typical silk I conformation (*41*). Asakura et al. (*34*) proposed on the basis of ^{13}C solid-state NMR that the silk I has multiple β-turns, while Zhou et al. (*42*) assigned it to a 3_1-helix-like structure based on density functional theory (DFT) calculation for the chemical shifts. The peak at 1666 cm^{-1} was highest in the membrane prepared at the lowest pH (Figure 1a), suggesting that low pH favors β-sheet formation in silk fibroin.

Both synchronous and asynchronous 2D Raman correlation spectra corresponding to a pH decrease from 8.0 to 5.2 clearly confirmed the existence of peaks at 1645, 1655, 1666, and 1685 cm^{-1} (see Figure 2). There was a strong autopeak (defined when $\nu_1 = \nu_2$ in cross-peak $\psi(\nu_1,\nu_2)$) centered at 1666 cm^{-1} and a weak autopeak centered at 1655 cm^{-1} on the diagonal, along with two negative cross-peaks at (1685, 1655) cm^{-1} and (1666,1645) cm^{-1} above the diagonal in the synchronous spectrum (Figure 2A). Although the 2D Pocha analysis software required an equal increment of, for example, pH or Ca^{2+} concentration to stack the individual 1D spectra to form a 2D map, our 2D Raman spectrum stacked without this requirement gave an identical result with that from 1D spectra. This implies that our 2D Raman correlation spectrum could be used to provide a qualitative analysis of the components in our samples. Based on the theory of generalized two-dimensional correlation spectroscopy (*38*), the results indicated that the 1666 cm^{-1} peak was very sensitive to pH change. The negative cross-peak, (1666, 1645) cm^{-1}, in the synchronous spectrum indicated that the component of peak 1666 cm^{-1} increased in parallel with a reduction in the 1645 cm^{-1} peak as pH values decreased. Similarly, the 1685 cm^{-1} peak increased as the 1655 cm^{-1} peak decreased. The 1645 cm^{-1} peak is often considered to arise from the α-helix conformation in some proteins or polypeptides (*43*, *44*). However, previous studies (*2*, *45*) demonstrated that there was little of α-helix conformation existing in native *Bombyx mori* silk fibroin solutions, so we inferred that the 1645 cm^{-1} peak might originate from a silk I-related state or an intermediate between random coil and silk I conformation. The 1685 cm^{-1} peak might arise from a silk II-related state, such as distorted β-sheet (*34*, *46*), or an intermediate between random coil and silk II conformation. There were at least three positive cross-peaks (1685, 1666), (1666,1655), and (1655,1645) cm^{-1} in the region from 1700 to 1630 cm^{-1} above the diagonal in asynchronous 2D Raman correlation spectra (Figure 2B). A positive asynchronous cross-peak $\psi(\nu_1,\nu_2)$ above the diagonal indicated that the bands ν_1 and ν_2 varied out of phase with each other and the band ν_1 changed prior to the band ν_2. The absence of such a peak suggested that the bands ν_1 and ν_2 changed synchronously based on the Noda theory (*38*). Therefore, our results shown in the asynchronous spectrum (Figure 2B) indicated that two conformations corresponding to the individual cross-peaks did not change simultaneously with a reduction in pH and there was a delay time between these two conformational changes. For these cross-peaks, the conformations represented by the following peaks changed in the following sequence as pH was decreased: 1685 → 1666 → 1655 → 1645 cm^{-1}. The silk II related intermediate (1685 cm^{-1}) and the typical silk II β-sheet conformation (1666 cm^{-1}) were the first to be induced as pH was decreased. Thus these in vitro observations suggested that in vivo a reduction in pH in the silkworm's duct might help to convert the random coil to β-sheet during the formation of the silk thread.

Table 1: Summary of the Deconvolution Results of ^{13}C NMR Spectra for the Membranes Prepared from Fibroin Solutions at Different pH Values

conformations	relative conformation contents (%)[a]			
	pH 5.2	pH 6.6	pH 6.9	pH 8.0
typical silk I (a)	61	77	71	71
typical silk II (b)	27	14	17	15
silk II-related intermediate (c)	7	4	5	5
silk I-related intermediate (d)	5	5	7	9
total silk I (a + d)	66	82	78	80
total silk II (b + c)	34	18	22	20

[a] The relative error in all reported conformation contents is less than 2%.

^{13}C CP-MAS solid-state NMR was used to analyze the pH-induced conformation changes in the fibroin membranes quantitatively. Figure 3 shows the experimental and simulated spectra together with the deconvoluted traces. The magnetic resonance of alanine C_β gave four dominant components in the region from 10 to 25 ppm, identifying the presence of four conformations determined in 1D and 2D Raman spectra. In general, alanine residues of silk I-related conformations or random coil conformation give chemical shifts from 14.5 to 17.5 ppm, while those of silk II give shifts from 18.5 to 21.5 (*42*). Our previous work (*42*) using density functional theory showed that the chemical shift around 17.0 ± 0.5 ppm corresponds to a typical silk I conformation with peptide torsion angles of $\langle\varphi\rangle = -59° \pm 2°$, $\langle\psi\rangle = 119° \pm 2°$, and $\langle\omega\rangle = 178° \pm 2°$ for alanine residues and $\langle\varphi\rangle = -78° \pm 2°$, $\langle\psi\rangle = 149° \pm 2°$, and $\langle\omega\rangle = 178° \pm 2°$ for glycine residue. These torsion angles fit a 3_1-helix-like structure, while the chemical shift around 20.0 ± 0.5 ppm fits the typical silk II (β-sheet) conformation (*35*, *47*−*50*) with peptide torsion angles of $\langle\varphi\rangle = -143° \pm 6°$, $\langle\psi\rangle = 142° \pm 5°$, and $\langle\omega\rangle = 178° \pm 2°$ for both alanine and glycine residues. The chemical shift at 15.0 ± 0.5 ppm possibly arose from random coil conformation, which we assigned to a silk I-related intermediate in the present paper. We also assigned the shift at 21.5 ± 0.5 ppm to a silk II-related intermediate, possibly a distorted β-sheet conformation. Table 1 shows the content for every component extracted from the deconvoluted traces. The total silk II content (including typical silk II and silk II-related intermediate) was higher (34%) at a pH of 5.2 than that at pH of 6.9 (22%) and 8.0 (20%) and that of unbuffered regenerated silk fibroin (18%) prepared (see methods section) at a pH of 6.6.

In the *Bombyx mori* silk gland, the pH of the silk dope falls from 6.9 to 4.8 as it flows from the posterior division to the distal part of the duct (*20*). This gradient in pH probably results from a proton pump found in the spinning duct (anterior part of the anterior division) (*51*) and a proton sink in the secretory part of the silk gland, which appears not to contain a highly active proton pump (Knight, D. P., personal communication). Our in vitro observations presented above suggested that the progressive reduction in pH in vivo may initiate a progressive increase in the β-sheet content in the fibroin as it flows from the posterior division through the spinning duct. They also suggested that the relatively high pH (6.9) found in the posterior gland that secretes and stores the fibroin provided a suitable environment for stabilizing this protein in the silk I or random coil conformation. A similar hypothesis has been advanced for the storage and β-sheet transformation in the natural formation of spider dragline silk (*52*). It is also of interest that Aggeli et al. (*53*) have demonstrated that protonation of a single glutamic acid carboxyl side chain in a short synthetic silk-like peptide could promote a transformation from an isotropic to a nematic liquid crystalline state. In this case, the reduction in charge produced by protonation of the carboxyl group presumably promoted aggregation by permitting the chains to approach closely enough to enable hydrophobic interactions between them. The mechanism by which a decrease in pH initiates the transformation from the silk I-like state to the silk II state in vitro and in vivo is not fully understood; however, reduction in negative charge by protonation of acidic amino acid side chains may promote a refolding to a more ordered state stabilized by hydrogen bonding between chains and accompanied by an exclusion of water (*27*). If a similar transformation occurred in the silk fibroin, the resulting orientation of the molecules and decrease in intermolecular distance could promote the formation of the silk II state. Such a mechanism could account for the nucleation dependency of the aggregation and secondary structural transformation of fibroin observed in vitro and postulated to occur in vivo (*54*). Thus dehydration may promote the formation of the silk II state. Conversely the addition of water may promote the formation of silk I by disrupting hydrogen bonds between chain segments (*55*).

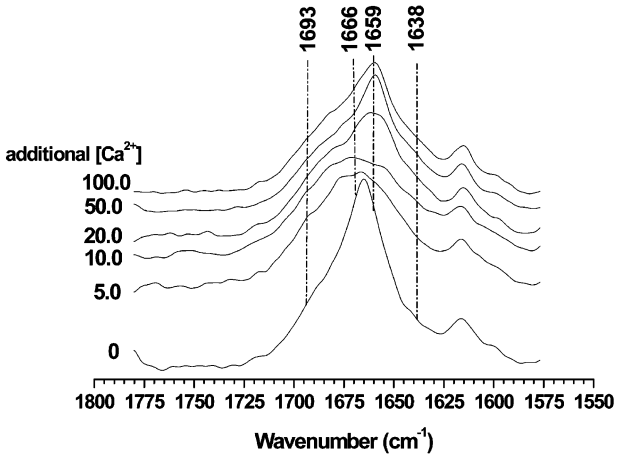

FIGURE 4: Raman spectra of a series of membranes prepared from regenerated fibroin solutions buffered at a pH 5.2 with the addition of 0, 5.0, 10.0, 20.0, 50.0, and 100.0 mg of Ca^{2+} per gram of fibroin.

Influence of Ca^{2+} on the Silk Fibroin Conformation. We used Raman spectroscopy and ^{13}C CP-MAS solid-state NMR spectroscopy to investigate the effect of Ca^{2+} ion concentration on the secondary structure formation in the fibroin membranes prepared at different pH values. Figure 4 shows the effect of different additional Ca^{2+} ion concentration (0, 5.0, 10.0, 20.0, 50.0, and 100.0 mg of Ca^{2+} per gram of fibroin) on the amide I region of the 1D Raman spectrum for the membranes prepared from the silk fibroin solution buffered to pH 5.2. Ca^{2+} ion concentration has a profound effect on the secondary structures present within the protein. 2D asynchronous Raman spectroscopy was used to identify the conformations most sensitive to the elevated Ca^{2+} ion concentrations (Figure 5). Figure 5A shows a broad band varying from 1700 to 1630 cm^{-1}. Figure 5B shows a slice trace at the wavenumber of 1659 cm^{-1} along the *x*-axis in the 2D map, which was highly sensitive to the changes in

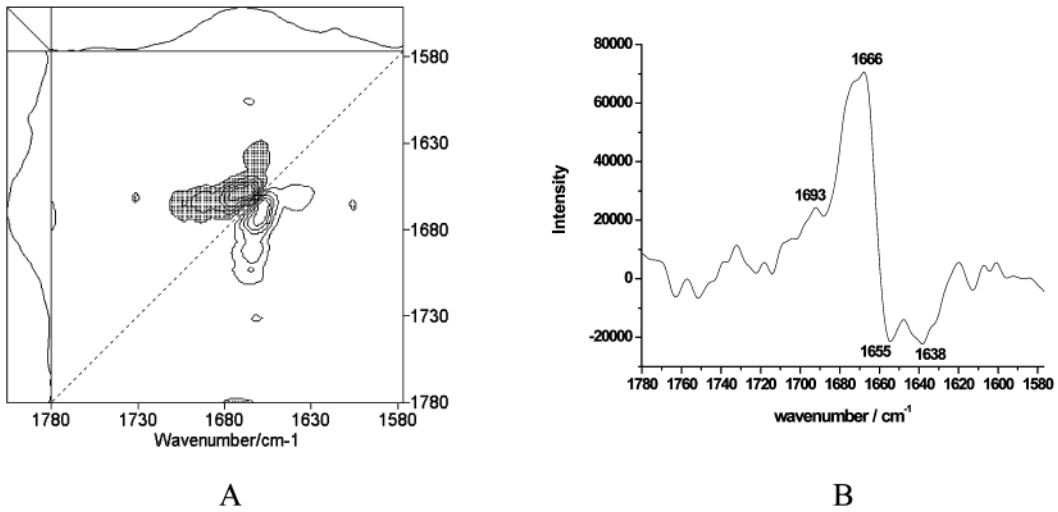

FIGURE 5: The effect of casting membranes from fibroin solutions at pH 5.2 with varied Ca^{2+} concentration (from 0 to 100.0 mg of Ca^{2+} per gram of fibroin): asynchronous 2D Raman correlation spectrum (A) and a single slice at 1659 cm^{-1} along the *x*-axis of the 2D map (B).

Ca^{2+} ion concentration. Four conformations represented by peaks 1693, 1666, 1655, and 1638 cm^{-1} changed with Ca^{2+} ion concentration in Figure 5B. The positive and negative intensities of peaks indicated different change in phase with the changes in Ca ion concentration during casting. The peaks 1685 and 1645 cm^{-1} seen in the membranes without additional Ca^{2+} ions shifted, respectively, to 1693 and 1638 cm^{-1} in membranes cast with additional Ca^{2+} ions possibly because of distortions produced by the binding of Ca^{2+} ion onto the fibroin. The peaks 1666 and 1655 cm^{-1} were still the most sensitive to the addition of Ca^{2+} ions (Figure 5B). A peak at >1680 cm^{-1} in amide I has often been observed in proteins and has been attributed to β-sheet (*56*), β-strand (*57*), and extended conformation (*58*). Because the contents of sensitive conformations changed bidirectionally with increase in Ca^{2+} ion concentration (Figure 4) contrasting with the unidirectional change with pH reduction, interpretation of cross-peaks in using out of phase theory (*38*) is not possible for the former.

Quantitative changes in the components produced by the different calcium concentrations were determined by the deconvolution of ^{13}C CP/MAS NMR spectra of alanine C_β (Figure 6 and Table 2). Also, four components were separated as in the above study. Total silk II contents (including typical silk II and its related intermediate) changed as Ca^{2+} ion concentration increased. The total silk II showed a maximum content (46%) when 10.0 mg of Ca^{2+} were added per gram of fibroin. A further increase in Ca^{2+} ion led to a progressive dramatic decrease in silk II falling at Ca^{2+} ion concentration of about 20 mg of Ca^{2+} per gram of fibroin even beneath that (34% total silk II) of control, which was lack of additional Ca^{2+} ions.

We also investigated the combined effects of changing pH and Ca^{2+} contents on the secondary structures of regenerated fibroin. The results of ^{13}C CP/MAS NMR of membranes prepared at pH 6.9 and 8.0 were summarized in Tables 3 and 4, respectively. Figure 7 summarizes the trends of total silk II conformations on the changes in different Ca^{2+} ion concentrations and pH values. The highest total silk II content was seen at 10 mg of Ca^{2+} per gram of fibroin at all three pH values studied. However at this level of Ca^{2+} addition, there was a progressive decrease in total silk II content with increase in pH: 46% at pH 5.2 (Figure 7a); 40% at pH 6.9 (Figure 7b); 37% at pH 8.0 (Figure 7c). Thus, as has been shown by Magoshi et al. (*20*) for native silk fibroin, our results for the regenerated fibroin showed that a low pH value favored the silk II conformation more than a neutral or alkaline one.

Furthermore, our results also showed that although a certain amount of additions of Ca^{2+} ion (≤ 10 mg of Ca^{2+} per gram of fibroin) promoted the silk II conformation, silk I-related conformations predominated even in the membranes prepared at the optimum pH (5.2) and optimum Ca^{2+} content (10 mg of Ca^{2+} per gram of fibroin) for silk II formation (see Table 2). This suggests that some additional factors such as extensional flow and wall shear and other metallic ions are required to complete the transition from silk I to silk II during natural spinning.

On the other hand, we observed that concentrations of Ca^{2+} ion ≥ 20 mg of Ca^{2+} per gram of fibroin partially prevented the formation of the silk II conformation (Figure 7). In the silkworm gland, Nemoto and co-workers (*30*) demonstrated a rereduction of the Ca^{2+} ion content in the anterior division of the spinning duct, resulting from outward diffusion or active transport. The rereduction of Ca^{2+} ion content could be necessary to promote the gel to sol transition for reducing the gel strength in native fibroin solutions and to permit it to flow through the spinning duct in the latter part of the secretory pathway (*20*, *29*, *30*). The relatively high Ca^{2+} ion concentration and elevated pH in the posterior and middle divisions compared with that in the anterior division of the gland lumen may promote a safe storage of the fibroin by helping to prevent the premature formation of silk II. Terry et al. (*59*) have made a similar suggestion. The authors thought that a higher concentration of Ca^{2+} ions could induce a gel formation (*59*). The immobilization of chains in the gel state within the early parts of the secretory pathway may prevent the chain movements required to form intermolecular β-sheets and therefore prevent the premature and irreversible formation of solid silk II. Safe storage of the silk protein may be further enhanced by the neutral pH (6.9) in these regions (*59*). In these circumstances, the low predicted isoelectric point (4.2) of heavy chain fibroin (*59*) may maintain a net negative charge on the molecules providing

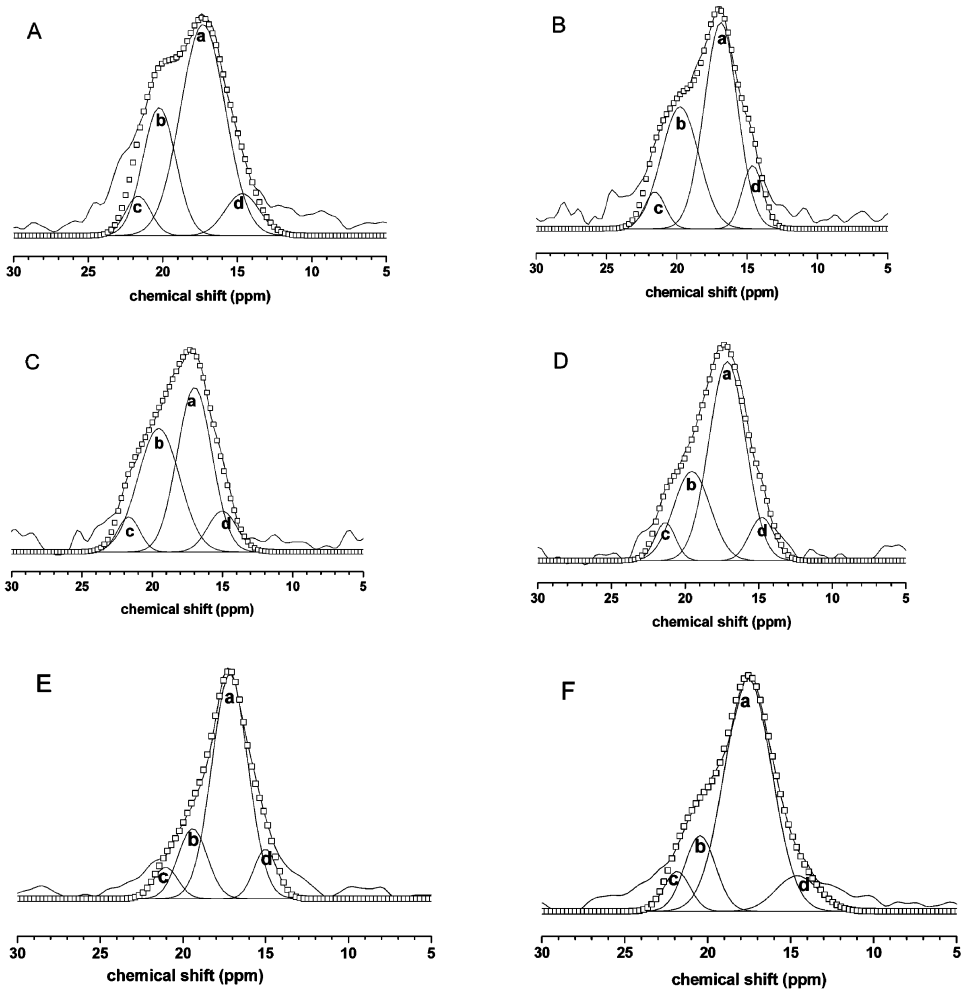

FIGURE 6: ^{13}C CP/MAS NMR spectra (solid line), simulated spectra (hollow squares), and their deconvoluted traces for alanine C_β. Panels A, B, C, D, E, and F are membranes prepared from regenerated fibroin at pH 5.2 fibroin buffer solution with additional Ca^{2+} ion concentrations of 0, 5.0, 10.0, 20.0, 50.0, and 100.0 mg of Ca^{2+} per gram of fibroin, respectively. Deconvolution gives typical silk I (17.0 ± 0.5 ppm, a), typical silk II (20.0 ± 0.5 ppm, b), silk II-related intermediate (21.5 ± 0.5 ppm, c), and silk I-related intermediate (15.0 ± 0.5 ppm, d).

Table 2: Summary of the Deconvolution Results of ^{13}C NMR Spectra for the Membranes Prepared at pH 5.2 from Regenerated Silk Fibroin Solutions with Different Ca^{2+} Ion Contents

additional Ca^{2+} (mg of Ca^{2+} per gram of fibroin) into regenerated silk fibrion	relative conformation contents (%)[a]				total silk I	total silk II
	typical silk I (a)	typical silk II (b)	silk II-related intermediate (c)	silk I-related intermediate (d)	(a + d)	(b + c)
0	58	27	7	8	66	34
5.0	51	34	6	9	60	40
10.0	44	40	6	10	54	46
20.0	59	26	6	9	68	32
50.0	67	18	6	9	76	24
100.0	68	15	6	9	79	21

[a] The relative error in all reported conformation contents is less than 2%.

more sites for the ionic binding or coordination of Ca^{2+} ions thus enhancing its stabilizing action for silk I-related conformations.

Ca^{2+} ions are known to play an important role in conformational change of many other proteins (*60*−*62*). For example, fibrinogen is a flexible molecule, and its conformation and flexibility are influenced by the Ca^{2+} ion concentration (*60*). These effects in fibrinogen are mediated through Ca^{2+} binding to low-affinity sites. The C-terminal region of the fibrinogen [A]α chain is more exposed at higher Ca^{2+} concentrations creating a molecule that is more liable to form intermolecular interactions. Lilie et al. (*61*) studied a repeated glycine-rich motif GGXGXDX(L/F/I)X in the N terminus of the secreted fibrinogen, which acts as the Ca^{2+} ligand. It formed a parallel β-helix (parallel β-roll), where the first six residues of each motif form a turn that bound Ca^{2+} ion and the remaining three residues build a short β-strand. The consecutive β-strand chains are connected in such a way that a right-handed helix of parallel β-strands is formed. One turn of this helix consists of two consecutive nine-residue motifs. The highly regular super-secondary structure of the parallel β-roll is dependent on the bound Ca^{2+} ions. A further

Table 3: Summary of the Deconvolution Results of ^{13}C NMR Spectra for the Membranes Prepared at pH 6.9 from Regenerated Silk Fibroin Solutions with Different Ca^{2+} Ion Contents

additional Ca^{2+} (mg of Ca^{2+} per gram of fibroin) into regenerated silk fibrion	relative conformation contents (%)[a]				total silk I	total silk II
	typical silk I (a)	typical silk II (b)	silk II-related intermediate (c)	silk I-related intermediate (d)	(a + d)	(b + c)
0	71	17	5	7	78	22
5.0	62	21	14	3	65	35
10.0	54	23	17	5	59	41
20.0	56	25	14	5	61	39
50.0	62	10	19	8	70	30
100.0	67	10	16	7	74	26

[a] The relative error in all reported conformation contents is less than 2%.

Table 4: Summary of the Deconvolution Results of ^{13}C NMR Spectra for the Membranes Prepared at pH 8.0 from Regenerated Silk Fibroin Solutions with Different Ca^{2+} Ion Contents

additional Ca^{2+} (mg of Ca^{2+} per gram of fibroin) into regenerated silk fibrion	relative conformation contents (%)[a]				total silk I	total silk II
	typical silk I (a)	typical silk II (b)	silk II-related intermediate (c)	silk I-related intermediate (d)	(a + d)	(b + c)
0	72	15	5	8	80	20
5.0	60	23	8	9	69	31
10.0	55	28	9	8	63	37
20.0	63	13	20	4	67	33
50.0	64	8	17	11	75	25
100.0	76	5	16	3	79	21

[a] The relative error in all reported conformation contents is less than 2%.

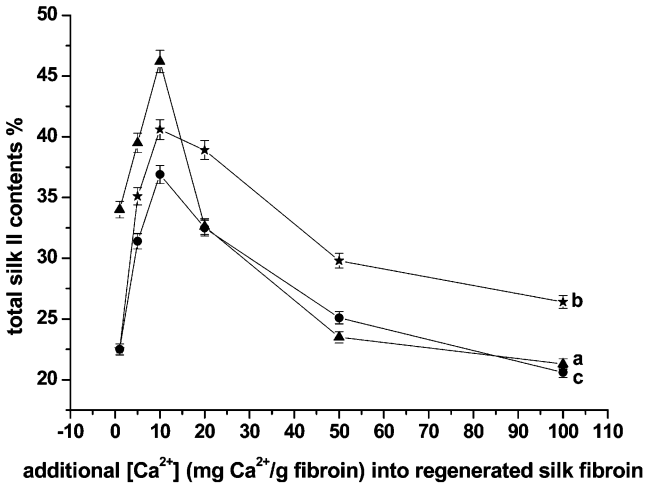

FIGURE 7: Dependence of total silk II conformations in silk fibroin membranes cast at different Ca^{2+} ion concentrations and pH values. Lines a, b, and c represent total silk II conformation at pH 5.2, 6.9, and 8.0, respectively. The relative error in all reported conformation contents is less than 2%.

example of a protein of which the conformation is dependent on calcium binding is the Alzheimer-linked neural protein S100B, a member of the EF-hand calcium binding proteins (*62*). Ca^{2+} binds to S100B with two loops causing a conformation change that exposes a hydrophobic surface allowing target peptides to bind by hydrophobic interactions to two exposed α-helices. Combining the way in which calcium ions induce secondary structure transitions in these nonsilk proteins with the highly repetitive -GAGAGS- motif of silk fibroin and its sensitivity to pH and Ca^{2+} ion, we suggest that Ca^{2+} ions might promote the silk II conformation by binding to the fibroin causing it to adopt a β-turn conformation. Alternatively Ca^{2+} ions might promote the formation of a 3_1-helix-like structure linking two β-strand chains and promoting β-sheet formation between them. Ca^{2+} might produce these structural transitions by disrupting the hydrogen bonds in silk fibroin chains lacking an ordered secondary structure thereby allowing freer chain movement to facilitate chain refolding. Because there is wide binding selectivity of Ca^{2+} to many amino acids in the protein, we are not sure at present which amino acids in the silk fibroin, a protein with 5263 amino acid residues and ~390 kDa molecular weigh for its heavy chain (*1*), are more preferable to the Ca^{2+} binding resulting in the formation of silk II conformation. Since the calcium content (1040 ± 46 ppm per gram of fibroin) in the regenerated silk fibroin is much higher than other metal elements, such as K (255 ± 73 ppm per gram of fibroin), Cu (18 ± 2 ppm per gram of fibroin), and Zn (13 ± 1 ppm per gram of fibroin) (*25*), the amino acids that are likely to coordinate Ca^{2+} may have a higher ratio in the silk fibroin. These amino acids may involve glycine, alanine, serine, tyrosine, valine, etc. being of higher ratio (*1*). However, we did not find a significant change in the fluorescence spectra at a range of 290−400 nm excited at 274 nm typical of the tyrosine residue when Ca^{2+} content was changed (data not shown). This indicates that the tyrosine may not be involved into the coordination with Ca^{2+}. The conformation sensitivity to the pH and Ca^{2+} content may imply that the Ca^{2+} binding sites in the silk fibroin are dependent on these conditions. The further work that we will undertake is to study the Ca^{2+} binding mechanism and binding ratio in the silk fibroin by using the model peptides.

In conclusion, we have demonstrated that the conformation conversion of regenerated silk fibroin is dependent on the pH and Ca^{2+} ion concentration. A lower pH (5.2) and a

certain amount of Ca^{2+} ions (10 mg of Ca^{2+} per gram of fibroin) favored the formation of silk II and silk II-related intermediate. These results, although still lacking structural analysis in detail, may help to account for the role of pH and Ca^{2+} ions in the natural spinning process of silkworms. We have also demonstrated that higher concentrations of Ca^{2+} ions partially inhibited the formation of silk II-related conformation probably by introducing strong electrostatic interaction between molecular chains. On the other hand, the relatively higher Ca^{2+} ion concentrations in the posterior division and middle part of the middle division than that in the anterior part of the middle division in the silkworm gland may prevent premature β sheet formation. In addition, a subsequent redecrease in Ca^{2+} in the anterior division may produce a sol form of the fibroin allowing it to flow through the duct. This together with the application of strain, the secretion of other ions, such as K^+, Mg^{2+}, and Cu^{2+} ions, etc., as well as the removal of water, may encourage more the formation of silk II-related conformations and the consequent formation of a solid silk. Thus our results may have important implications for understanding the natural silk spinning process and how that may be mimicked to produce useful materials. Finally, our results suggest that regenerated silk fibroin may be a useful model system for studying the role of Ca^{2+} ions and pH in controlling the aggregation, orientation, and formation of intermolecular β-sheets in clinically important proteins such as those of prions and amyloid.

ACKNOWLEDGMENT

The ^{13}C solid-state NMR experiments in this work were performed in the State Key Laboratory of Magnetic Resonance and Atomic and Molecular Physics, Wuhan Institute of Physics & Mathematics, the Chinese Academy of Sciences. We thank Profs. Ye, Chaohui, and Liu, Maili, in the State Key Laboratory for access to their Infinityplus 400 NMR spectrometer and other facilities for experiments. In addition, we thank Prof. Wu, Peiyi, who guided us kindly on how to use the 2D Raman software.

REFERENCES

1. Zhou, C. Z., Confalonieri, F., Medina, N., Zivanovic, Y., Esnault, C., Yang, T., Jacquet, M., Janin, J., Duguet, M., Perasso, R., and Li, Z. G. (2000) Fine organization of *Bombyx mori* fibroin heavy chain gene, *Nucleic Acids Res. 28*, 2413−2419.
2. Asakura, T., Suzuki, H., and Watanabe, Y. (1983) Conformational characterization of silk fibroin in intact *Bombyx mori* and *Philosamia cynthia ricini* silkworms by ^{13}C NMR spectroscopy, *Macromolecules 16*, 1024−1026.
3. Krejchi, M. T., Cooper, S. J., Deguchi, Y., Atkins, E. D. T., Fournier, M. J., Mason, T. L., and Tirrell, D. A. (1997) Crystal structures of chain-folded antiparallel beta-sheet assemblies from sequence-designed periodic polypeptides, *Macromolecules 30*, 5012−5024.
4. Panitch, A., Matsuki, K., Cantor, E. J., Cooper, S. J., Atkins, E. D. T., Fournier, M. J., Mason, T. L., and Tirrell, D. A. (1997) Poly(L-alanylglycine): Multigram-scale biosynthesis, crystallization, and structural analysis of chain-folded lamellae, *Macromolecules 30*, 42−49.
5. Jones, N. A., Sikorski, P., Atkins, E. E. T., and Hill, M. J. (2000) Nature and structure of once-folded nylon 6 monodisperse oligoamides in lamellar crystals, *Macromolecules 33*, 4146−4154.
6. Asakura, T., Watanabe, Y., and Itoh, T. (1984) NMR of silk fibroin. 3. Assignment of carbonyl carbon resonances and their dependence on sequence and conformation in *Bombyx mori* silk fibroin using selective isotopic labeling, *Macromolecules 17*, 2421−2426.
7. Shao, Z., Vollrath, F., Sirichaisit, J., and Young, R. J. (1999) Analysis of spider silk in native and supercontracted states using Raman spectroscopy, *Polymer 40*, 2493−2500.
8. Gosline, J. M., DeMont, M. E., and Denny, M. W. (1986) The Structure And Properties Of Spider Silk, *Endeavour 10*, 37−43.
9. Tirrell, D. A. (1996) Putting a new spin on spider silk, *Science 271*, 39−40.
10. Shao, Z. Z., and Vollrath, F. (2002) Materials: Surprising strength of silkworm silk, *Nature 418*, 741.
11. Cappello, J., Crissman, J., Dorman, M., Mikolajczak, M., Textor, G., Marquet, M., and Ferrari, F. (1990) Genetic-engineering of structural protein polymers, *Biotechnol. Prog. 6*, 198−202.
12. McGrath, K. P., Tirrell, D. A., Kawai, M., Masson, T. L., and Fournier, M. J. (1990) Chemical and biosynthetic approaches to the production of novel polypeptide materials, *Biotechnol. Prog. 6*, 188−192.
13. Asakura, T., Nitta, K., Yang, M. Y., Yao, J. M., Nakazawa, Y., and Kaplan, D. L. (2003) Synthesis and characterization of chimeric silkworm silk, *Biomacromolecules 4*, 815−820.
14. Lazaris, A., Arcidiacono, S., Huang, Y., Zhou, J., Duguay, F., Chreien, N., Welsh, E. A., Soares, J. W., and Karatzas, C. N. (2002) Spider silk fibers spun from soluble recombinant silk produced in mammalian cells, *Science 295*, 472−476.
15. Putthanarat, S., Zarkoob, S., Magoshi, J., Chen, J. A., Eby, R. K., Stone, M., and Adams, W. W. (2002) Effect of processing temperature on the morphology of silk membranes, *Polymer 43*, 3405−3413.
16. Putthanarat, S., Stribeck, N., Fossey, S. A., Eby, R. K., and Adams, W. W., (2000) Investigation of the nanofibrils of silk fibers, *Polymer 41*, 7735−7747.
17. Seidel, A., Liivak, O., and Jelinski, L. W. (1998) Artificial spinning of spider silk, *Macromolecules 31*, 6733−6737.
18. Seidel, A., Liivak, O., Calve, S., Adaska, J., Ji, G., Yang, Z., Grubb, D., Zax, D., and Jelinski, L. (2000) Regenerated spider silk: Processing, properties, and structure, *Macromolecules 33*, 775−780.
19. Knight, D. P., and Vollrath, F. (2001) Changes in element composition along the spinning duct in a Nephila spider, *Naturwissenschaften 88*, 179−182.
20. Magoshi, J., Magoshi, Y., and Nakamura, S. (1994) Mechanism of fiber formation of silkworm, *ACS Symp. Ser. 544*, 292−310.
21. Zheng, S. D., Li, G. X., Yao, W. H., and Yu, T. Y. (1989) Raman-spectroscopic investigation of the denaturation process of silk fibroin, *Appl. Spectrosc. 43*, 1269.
22. Liivak, O., Blye, A., Shah, N., and Jelinski L. W. (1998) A microfabricated wet-spinning apparatus to spin fibers of silk proteins. Structure−property correlations, *Macromolecules 31*, 2947−2951.
23. Chen, X., Knight, D. P., and Vollrath, F. (2002) Rheological characterization of *Nephila* spidroin solution, *Biomacromolecules 3*, 644−648.
24. Chen, X., Knight, D. P., Shao, Z. Z., and Vollrath, F. (2002) Conformation transition in silk protein films monitored by time-resolved Fourier transform infrared spectroscopy: Effect of potassium ions on *Nephila* spidroin films, *Biochemistry 41*, 14944−14950.
25. Li, G., Zhou, P., Sun, Y., Yao, W., Mi, Y., Yao, H., Shao, Z., and Yu, T. (2001) The effect of metal ions on the conformation transition of silk fibroin, *Chem. J. Chin. Univ. 22*, 860−862.
26. Thiel, B. L., and Viney, C. (1997) Spider major ampullate silk (drag line): Smart composite processing based on imperfect crystals, *J. Microsc. (Oxford) 185* (Part 2), 179−187.
27. Magoshi, J., Magoshi, Y., Becker, M. A., and Nakamura, S. (1996) Silk Fiber Formation, Multiple Spinning Mechanisms, in *Polymeric Materials Encyclopedia* (Salamone, Joseph C., Ed.), CRC Press, Boca Raton, FL.
28. Thiel, B. L., Kunkel, D. D., and Viney, C. (1994) Physical and chemical microstructure of spider dragline − a study by analytical transmission electron-microscopy, *Biopolymers 34*, 1089−1097.
29. Ochi, A., Hossain, K. S., Magoshi, J., and Nemoto, N. (2002) Rheology and dynamic light scattering of silk fibroin solution extracted from the middle division of *Bombyx mori* silkworm, *Biomacromolecules 3*, 1187−1196.
30. Hossain, K. S., Ochi, A., Ooyama, E., Magoshi, J. and Nemoto, N. (2003) Dynamic light scattering of native silk fibroin solution extracted from different parts of the middle division of the silk gland of the *Bombyx mori* silkworm, *Biomaromolecules 4*, 350−359.

31. Monti, P., Freddi, G., Bertoluzza, A., Kasai, N., and Tsukada, M. (1998) Raman spectroscopic studies of silk fibroin from *Bombyx mori*, *J. Raman Spectrosc. 29*, 297−304.
32. Monti, P., Taddei, P., Freddi, G., Asakura, T., and Tsukada, M. (2001) Raman spectroscopic characterization of *Bombyx mori* silk fibroin: Raman spectrum of Silk I, *J. Raman Spectrosc. 32*, 103−107.
33. Asakura, T., Kuzuhara, A., Tabeta, R., and Saito, H. (1985) Conformation characterization of bombyx-mori silk fibroin in the solid-state by high-frequency C-13 cross polarization magic angle spinning nmr, X-ray-diffraction, and infrared-spectroscopy, *Macromolecules 18*, 1841−1845.
34. Asakura, T., Yao, J., Yamane, T., Umemura, K., and Ulrich, A. S. (2002) Heterogeneous structure of silk fibers from *Bombyx mori* resolved by C-13 solid-state NMR spectroscopy, *J. Am. Chem. Soc. 124*, 8794−8795.
35. Asakura, T., and Yao, JM. (2002) C-13 CP/MAS NMR study on structural heterogeneity in *Bombyx mori* silk fiber and their generation by stretching, *Protein Sci. 11*, 2706−2713.
36. Asakura, T., Sugino, R., Yao, J., Takashima, H., and Kishore, R., (2002) Structural analysis of semicrystalline *Bombyx mori* silk fibroin chain with silk I and silk II forms by 13C, 15N and 2H stable isotope labeling, conformation-dependent chemical shifts and solid-state NMR spectroscopy, *Biochemistry 41*, 4415−4424.
37. Brame, E. G., and Grasselli, J. G. (1977) *Infrared and Raman Spectroscopy; Part C*, Marcel Dekker, New York.
38. Noda, I. (1993) Generalized 2-dimensional correlation method applicable to infrared, Raman, and other types of spectroscopy, *Appl. Spectrosc. 47*, 1329−1336.
39. Jiang, H. J., Wu, P. Y., and Yang, Y. L. (2003) Variable temperature FTIR study of poly(ethylene-*co*-vinyl alcohol)-*graft*-poly(epsilon-caprolactone), *Biomacromolecues 4*, 1343−1347.
40. Peng, Y.; Wu, P. Y., and Yang, Y. L. (2003) Two-dimensional infrared correlation spectroscopy as a probe of sequential events in the diffusion process of water in poly(epsilon-caprolactone), *J. Chem. Phys. 119*, 8075−8079.
41. Liu, Y. C., Shao, Z. Z., and Sun, Y. Yu. (1998) Structure and function of *B. mori* silk fibroin, *Polym. Bull. 3*, 17−23.
42. Zhou, P., Li, G. Y., Shao, Z. Z., Pan, X. Y., and Yu, T. Y. (2001) Structure of *Bombyx mori* silk fibroin based on the DFT chemical shift calculation, *J. Phys. Chem. B. 105*, 12469−12476.
43. Kubelka, J., Pancoska, P., and Keiderling, T. A. (1999) Novel Use of a Static Modification of Two-Dimensional Correlation Analysis. Part II: Hetero-Spectral Correlations of Protein Raman, FT-IR, and Circular Dichroism Spectra, *Appl. Spectrosc. 53*, 666−671.
44. Etori, H., Yamada, Y., Taga, K., Okabayashi, H., Ohshima, K., and O′Connor, C. J. (1997) Raman scattering study of *N*-acyl-L-alanine oligomer salts: Stabilization of the α-helical structure promoted by micellization, *Vib. Spectrosc. 14*, 133−141.
45. Asakura, T. (1986) NMR of silk fibroin.6. Structure of bombyx-mori silk fibroin in aqueous-solution, *Makromol. Chem., Rapid Commun. 7*, 755−759.
46. Tuma, R., Prevelige, P. E., Jr., and Thomas, G. J., Jr. (1996) Structural Transitions in the Scaffolding and Coat Proteins of P22 Virus during Assembly and Disassembly, *Biochemistry 35*, 4619−4627.
47. Ochsenfeld, C., Brown, S. P., Schnell, I., Gauss, J. and Spiess, H. W. (2001) Structure Assignment in the Solid State by the Coupling of Quantum Chemical Calculations with NMR Experiments: A Columnar Hexabenzocoronene Derivative, *J. Am. Chem. Soc. 123*, 2597−2606.
48. Spera, S., and Bax A. (1991) Empirical correlation between protein backbone conformation and Cα and Cβ 13C nuclear magnetic resonance chemical shifts, *J. Am. Chem. Soc. 113*, 5490−5492.
49. Saitô, H., Tabeta, R., Shoji, A., Ozaki, T., and Ando, I. (1983) Conformational characterization of polypeptides in the solid state as viewed from the conformation-dependent carbon-13 chemical shifts determined by the carbon-13 cross polarization/magic angle spinning method: oligo(L-alanine), poly(L-alanine), copolymers of L- and D-alanines, and copolymers of L-alanine with *N*-methyl- or *N*-benzyl-L-alanine, *Macromolecules 16*, 1050−1057.
50. Asakura, T., Ashida, J., Yamane, T., Kameda, T., Nakazawa, Y., Ohgo, K., and Komatsu, K. (2001) A repeated β-turn structure in Poly(Ala-Gly) as a model for silk I of *Bombyx mori* silk fibroin studied with two-dimensional spin-diffusion NMR under off magic angle spinning and rotational echo double resonance, *J. Mol. Biol. 306*, 291−305.
51. Azuma, M., and Ohta, Y. (1998) Changes in H+-translocating vacuolar-type ATPase in the anterior silk gland cell of *Bombyx mori* during metamorphosis, *J. Exp. Biol. 201*, 479−486.
52. Vollrath, F., and Knight, D. P. (2001) Liquid crystalline spinning of spider silk, *Science 410*, 541−548.
53. Aggeli, A., Bell, M., Carrick, L. M., Fishwick, C. W. G., Harding, R., Mawer, P. J., Radford, S. E. Strong, A. E., and Boden, N. (2003) pH as a trigger of peptide beta-sheet self-assembly and reversible switching between nematic and isotropic phases, *J. Am. Chem. Soc. 125*, 9619−9628.
54. Li, G., Zhou, P., Shao, Z., Xie, X., Chen, X., Wang, H., Chunyu, L., and Yu, T. (2001) The natural silk spinning process − A nucleation-dependent aggregation mechanism? *Eur. J. Biochem. 268*, 6600−6606.
55. Pérez-Rigueiro, J., Viney, C., Llorca, J., and Elices, M. (2000) Mechanical properties of silkworm silk in liquid media, *Polymer 41*, 8433−8439.
56. Pelton, J. T., and Mclean, L. R. (2000) Spectroscopic Methods for Analysis of Protein Secondary Structure, *Anal. Biochem. 277*, 167−176.
57. Tuma, R., Prevelige, P. E., and Thomas, G. J. (1996) Structural Transitions in the Scaffolding and Coat Proteins of P22 Virus during Assembly and Disassembly, *Biochemistry 35*, 4619−4627.
58. Tuma, R., Parker, M. H., Weigele, P., Sampson, L., Sun, Y., Krishna, R., Casjens, S., Thomas, G. J., and Prevelige, P. E. (1998) A helical coat protein recognition domain of the bacteriophage P22 scaffolding protein, *J. Mol. Biol. 281*, 81−94.
59. Terry, A. E., Knight, D. P., Porter, D., and Vollrath, F. (2004) pH induced Changes in the Rheology of Silk Solution from the Middle Division of *Bombyx mori* Silkworm, *Biomacromolecules 5*, 768−772.
60. Apap-Bologna, A., Webster, A., Raitt, F., and Kemp, G. (1989) The influence of calcium ions on fibrinogen conformation, *Biochim. Biophys. Acta 995*, 70−74.
61. Lilie, H., Haehnel, W., Rudolph, R., and Baumann, U. (2000) Folding of a synthetic parallel β-roll protein, *FEBS Lett. 470*, 173−177.
62. McClintock, K. A., and Shaw, G. S. (2003) A Novel S100 Target conformation is revealed by the solution structure of the Ca−S100B-TRTK-12 complex, *J. Biol. Chem. 278*, 6251−6257.

BI049344I